JOURNAL OF Materials CHEMISTRY

Synthesis and characterization of multiwalled carbon nanotubes produced using zeolite Co-beta

G. Kamalakar, Dennis W Hwang and Lian-Pin Hwang*

Department of Chemistry, National Taiwan University And Institute of Atomic and Molecular Sciences, Academia Sinica, P.O.Box, 23-24 Taipei, Taiwan, Republic of China.
E-mail: nmra@po.iams.sinica.edu.tw

Received 26th November 2001, Accepted 2nd April 2002
First published as an Advance Article on the web 25th April 2002

Multiwalled carbon nanotubes are synthesized using Co-beta for the first time using the catalytic chemical vapour deposition method. The effects of reaction temperature, reaction time, and flow rate of acetylene on the growth of multiwalled carbon nanotubes are studied. From the TEM results it is established that the growth of multiwalled carbon nanotubes follows a tip growth mechanism. To understand the magnetic behavior of the Co, which is present at the tip of the nanotubes, magnetic measurements are performed using a SQUID magnetometer and the results are discussed.

Introduction

From the time of the discovery of carbon nanotubes by Ijima,[1] in the year 1993, there has been explosive growth in the field of synthesis and applications of nanotubes. Electric arc discharge, laser vaporization, electrolysis, synthesis from bulk polymer, solid pyrolysis, and *in situ* catalysis are the techniques which have been employed over the years for the synthesis of carbon nanotubes.[2–10] However in recent years the catalytic chemical vapour deposition method using solid supports like silica and molecular sieves such as Y or APO-5 have received greater attention for the efficient synthesis of carbon nanotubes.[11–15] The advantages of this method over the rest of the techniques are the milder reaction conditions for the synthesis of carbon nanotubes and the possible formation of very long nanotubes. Keeping these advantages in mind we have developed here a novel methodology for the synthesis of multiwalled carbon nanotubes (MWCNT) using zeolite beta as the support. Zeolites with well-defined pore structures and high surface areas have in general very good metal dispersion properties. In the growth of carbon nanotubes this dispersion of the metal catalyst over the support plays an important role. Only certain faces of the metal in specific orientation will assist the growth of well graphitized carbon nanotubes. In the present work we report here cobalt-modified zeolite beta as another candidate for the growth of multiwalled carbon nanotubes in the vapour phase. Some of the multiwalled carbon nanotubes made by this procedure are as long as 15 μm which may find potential applications in nanomolecular technology.

Experimental

Catalyst preparation

The catalytic support beta is synthesized using a procedure reported in the literature.[16] The cobalt metal particles are deposited over the surface of zeolite beta by the wet impregnation method. In this procedure the nitrate salt of this metal is dissolved in the required amount of water forming a homogenous mixture. Then zeolite powder of the required amount is added to it and thoroughly stirred for three hours. The resulting mixture is subjected to evaporation to give the Co-beta zeolite. This material is calcined at 400 °C for four hours and is used for the synthesis of multiwalled carbon nanotubes.

Synthesis of CNT

About 100 mg of the catalyst prepared by the above procedure is uniformly sprayed inside a ceramic boat. Then this boat is placed in the central part of a horizontal fixed bed quartz reactor tube and the tube is heated to 300 °C in a steady flow of nitrogen gas (100 sccm). After one hour the temperature of the reaction is further raised to the required temperature of synthesis (625–800 °C) and a controlled flow of acetylene (7.5–15 sccm) is introduced into the tube along with the carrier gas nitrogen (100 sccm) for a specific reaction time (45–120 minutes). After the completion of the reaction, the flow of acetylene is stopped and the tube is allowed to cool to room temperature in the flow of nitrogen. The effects of impregnating different amounts of cobalt over the zeolite beta were studied. The synthesis reaction of multiwalled carbon nanotubes was also studied using different metal ions like Fe, Co, Ni, Zn and Pd.

TEM

The carbon nanotubes so formed were studied by using transmission electron microscopy (TEM: Hitachi H-7100, 120 KV) after sonicating the samples in suitable amount of ethanol solvent for 30 minutes and then dispersing a drop of the resulting solution over a holey copper grid. The results are presented in Fig. 1 and Fig. 3. High resolution TEM pictures are presented in Fig. 2 and Fig. 5.

XRD

The XRD spectra were recorded using a Scintag (USA) XRD spectrometer with CuK_{α} radiation ($\lambda = 1.5418$ Å). The results are presented in Fig. 4.

Magnetic measurements

DC magnetic measurements were studied in the range of magnetic fields 5 to 20 KG and at temperatures 5, 100 and 300 K using a superconducting quantum interference device (SQUID) magnetometer. The results are presented in Figs. 6 to 8.

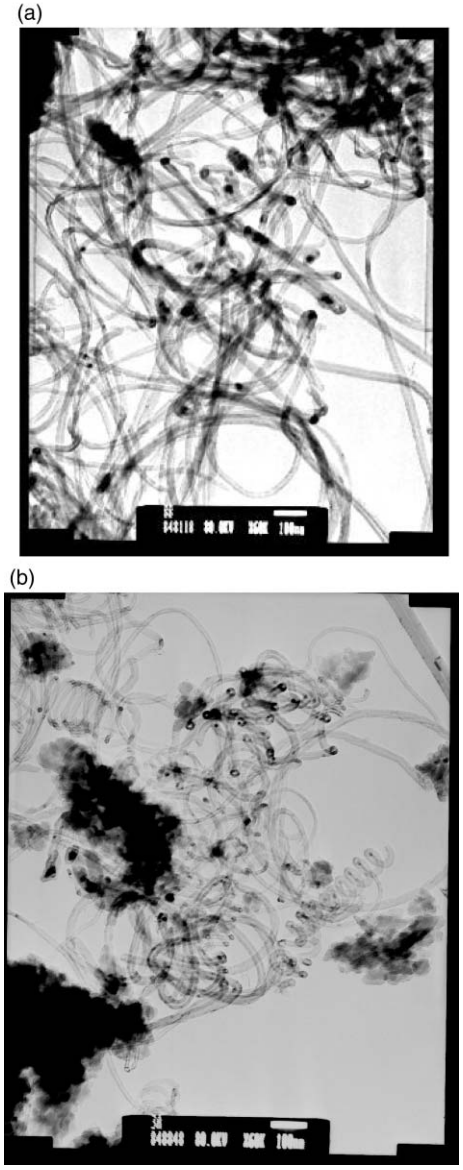

Fig. 1 TEM pictures of the multiwalled carbon nanotubes prepared at 700 °C, N_2 = 100 sccm, C_2H_2 = 10 sccm and Co-beta = 100 mg.

Results and discussion

Variation of reaction parameters

We have studied the effect of using different transition metals like Fe, Ni, Zn and rare earth element Pd in the synthesis of multiwalled carbon nanotubes. Well graphitized carbon nanotubes are observed only in the case of Co metal and hence further studies were carried out using that catalyst. Other reasons why we have chosen Co metal as catalyst are as follows. Co metal possesses a greater ability to produce more ordered carbon (graphitization ability), a greater ability to decompose unsaturated hydrocarbons like acetylene, and Co allows the decomposed carbon to diffuse rapidly through it resulting in metastable states of carbon which are essential for the formation of nanotubes, when compared with the other metal catalyst particles.[17–19] Impregnation of a 5% loading of cobalt over zeolite beta was chosen for the reaction optimization as higher loadings of cobalt did not yield any better results. The synthesis temperature, reaction time and flow rate of acetylene were optimized for Co-beta. The reaction temperature was varied from 625 to 800 °C and no nanotubes were formed at lower temperatures (<650 °C). However formation of the carbon nanotubes was observed from 675 °C onwards and the optimum temperature for the synthesis of carbon nanotubes

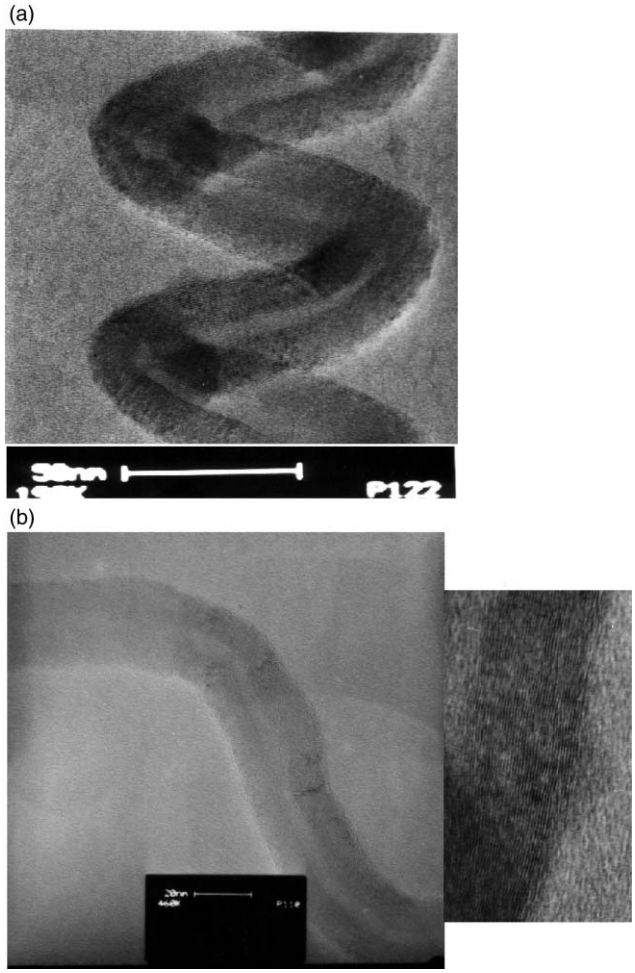

Fig. 2 HRTEM pictures of (a) helical multiwalled carbon nanotube, (b) normal multiwalled carbon nanotube (inset: multiwalls).

was found to be 700 °C. At higher reaction temperatures (>775 °C) more amorphous carbon was observed. Further at higher reaction temperatures the agglomeration of metal particles occurs, thus increasing the size of the metal particles. Larger metal particles are inactive towards the growth of the nanotubes and hence will lead to the formation of amorphous carbon. During these reactions the flow rates of nitrogen and acetylene were maintained constant at 100 and 10 sccm respectively.

The TEM pictures in Fig. 1 corresponds to the carbon nanotubes obtained under optimal reaction conditions. We also observed (Fig. 1b) some helical shaped multiwalled carbon nanotubes, which are present in much smaller quantities. Different mechanisms of nanotube formation using the CVD technique are described elsewhere in the literature.[20] High resolution TEM pictures of helical and normal multiwalled carbon nanotubes are presented in Fig. 2a and b. The presence of several multiwalls can be observed in the HRTEM pictures. The inner and outer diameters of these tubes are in the range of 12–13 nm (id) and 19–23 nm (od) respectively. The product obtained under the best reaction conditions of synthesis temperature (700 °C), flow of nitrogen (100 sccm) and acetylene (10 sccm) and reaction time (30 minutes) was treated repeatedly (5 times) with 50% hydrofluoric acid (RDH, Germany) and later with hydrochloric acid to remove the undissolved metal. The resulting sample was dried in vacuum and then heated in a flow of air (12 sccm) for two hours at 450 °C to remove amorphous carbon. The TEM picture of Fig. 3b shows the purified multiwalled carbon nanotubes. The TEM picture of nanotubes of length sevral nanometers obtained in the present study is presented in Fig. 3a.

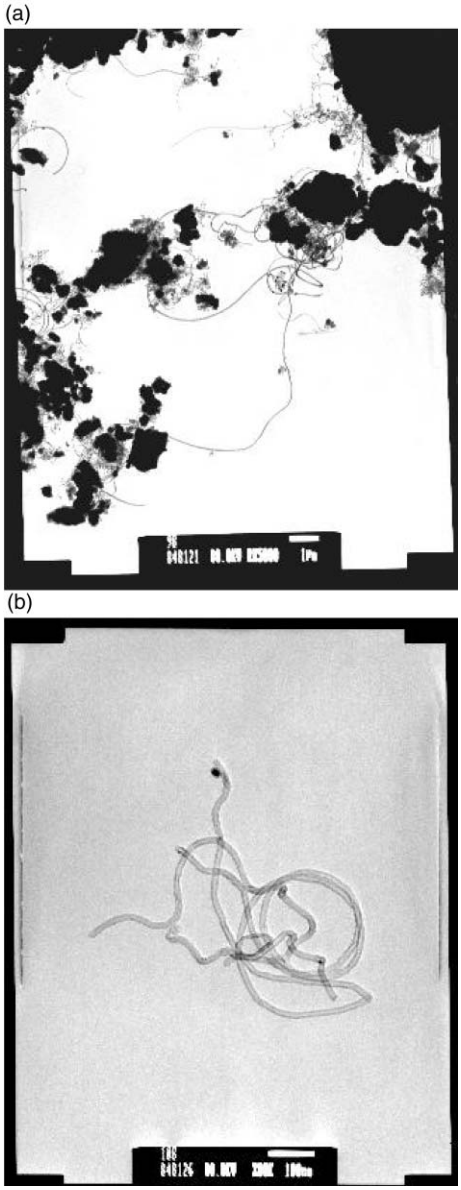

Fig. 3 TEM pictures of (a) a very long carbon nanotube, (b) multiwalled carbon nanotubes prepared at 700 °C, N_2 = 100 sccm, C_2H_2 = 10 sccm and Co-beta = 100 mg after purification.

The synthesis of nanotubes was also carried out at different reaction times and an optimum reaction time was observed to be 90 minutes. Though there could be higher carbon yields at longer reaction times, no increase in the yield of the carbon nanotubes was observed due to the deactivation of the catalyst metal particles by carbon saturation at longer reaction times. At higher flow rates of acetylene, amorphous carbon formation is predominant since it leads to the availability of excess carbon for the same amount of metal catalyst particles available for the graphitization purpose.

XRD

The XRD patterns of the acid treated sample, untreated sample and zeolite Co-beta are together given in Fig. 4. The complete removal of the zeolite beta support is observed from the XRD pattern of the acid treated sample. Peaks due to graphite (2θ = 26.33) and a very low intensity peak due to Co (2θ = 44.15) are also observed in the pattern of the acid treated sample. The cobalt peak may be due to the entrapped cobalt at the tips of these tubes.[21] A HRTEM picture in Fig. 5 demonstrates this fact.

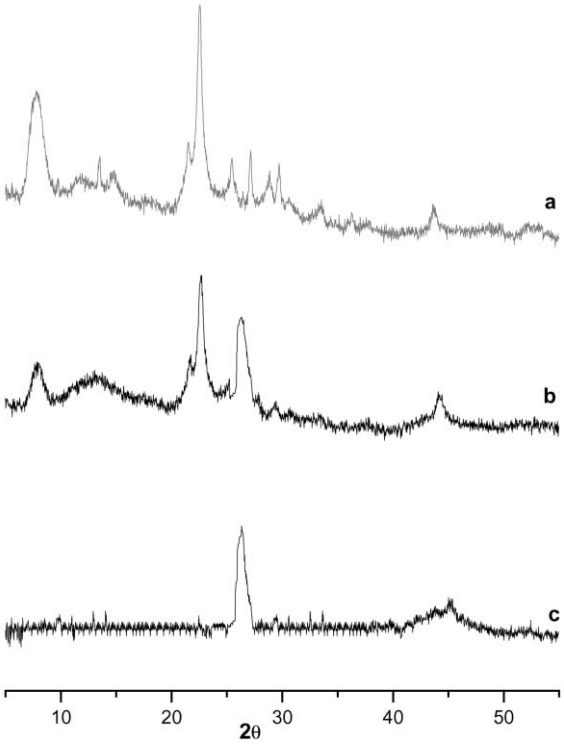

Fig. 4 XRD spectra of (a) zeolite Co-beta, (b) as synthesized MWCNT product, (c) acid treated sample.

Magnetic measurements

Since the MWCNTs have Co at their tips, the magnetic properties of these random nanotubes were measured using a SQUID magnetometer at 5,10 and 20 KG magnetic fields in the temperature range 5 to 300 K.

The magnetic hysteresis loops recorded at 5, 100 and 300 K are shown in Fig. 6. The nanotubes do show ferromagnetic behavior as expected and the temperature dependence of the hysteresis is also similar to those observed by others.[20,22] The temperature dependences of the ratio of M_r/M_s and the coercive field H_c extracted from the hysteresis loops, where M_r and M_s are the remnant and saturation magnetisation respectively, are shown in Fig. 7. It is observed that both the M_r/M_s ratio and the coercive field H_c decrease monotonically with increasing temperature, which is a characteristic of smaller particles. The values of M_r/M_s ratio and H_c obtained here were lower than those obtained for Fe nanotubes.[23] However, they are comparable to the values obtained in Co–carbon nanocrystalline films.[24] The ratio of M_r/M_s for randomly distributed easy-axis single domain particles is known to be $\sim$0.5 at a temperature well below the blocking temperature. Therefore the decrease in both M_r/M_s ratio and H_c with increasing temperature is attributed to the depinning of the domain walls in the particles.

The rate of decrease of the M_r/M_s ratio and H_c with temperature is also observed to be slower than that observed for Fe nanotubes. While M_r/M_s changes from about 0.6 to 0.3 in the temperature range 5 to 300 K for the Fe nanotubes, the variation for the same temperature range for Co nanotubes is only from about 0.46 to 0.3. Similarly the variation of H_c for Co tubes is in the range of 0.82 to 0.3 KOe, while for Fe nanotubes it was from 2 to 0.3 KOe.

Plots of magnetisation (emu g^{-1}) *versus* applied magnetic field at three different temperatures, namely, 5, 100 and 300 K are shown in Fig. 8. From the graph it is seen that the saturation magnetisation is almost independent of temperature and has a value of about 2 emu g^{-1} which is in accordance with earlier reports in the literature.[25]

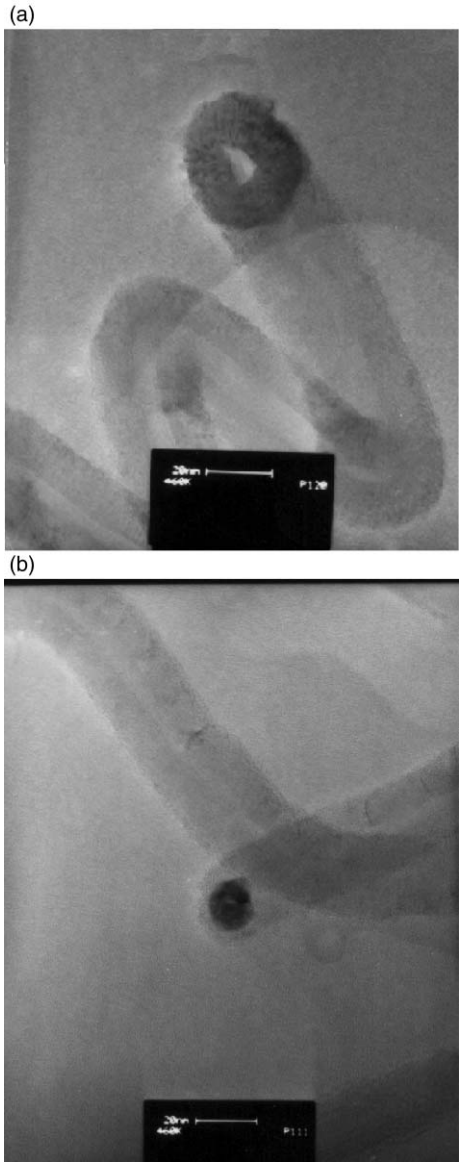

Fig. 5 HRTEM pictures of the cobalt metal particle entrapped at the tip of the tube (helical (a) and normal (b) multiwalled carbon nanotubes).

The good ferromagnetic behavior exhibited by these Co-nanotubes reinforces the possibility of making use of these nanotubes in commercial magnetic recording devices, apart from the promise they hold for other magnetic device applications.

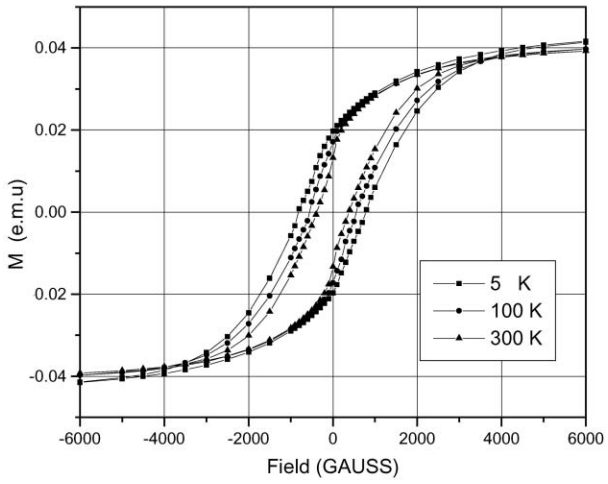

Fig. 6 Magnetic hysteresis loops at three different temperatures obtained using a SQUID magnetometer.

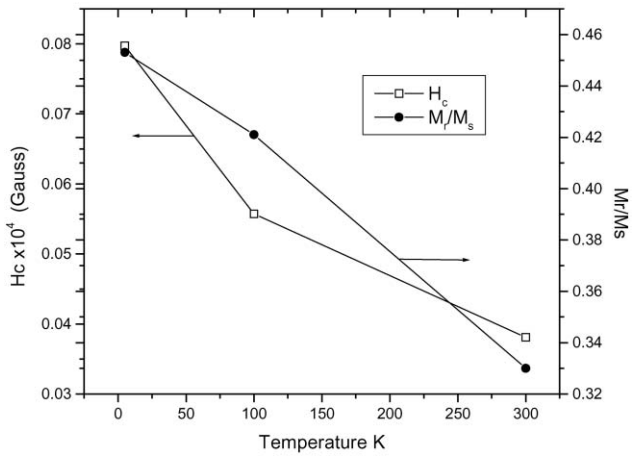

Fig. 7 Plots of the M_r/M_s ratio and coercive field H_c as a function of temperature.

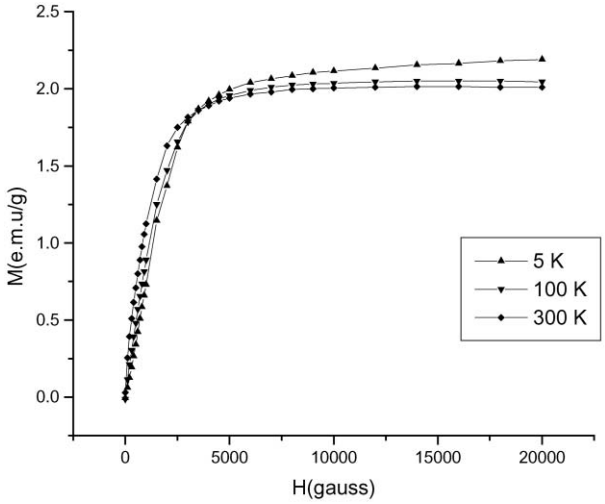

Fig. 8 Plots of magnetisation (emu g^{-1}) *versus* magnetic field at three different temperatures.

Growth mechanism

In general there are two plausible mechanisms,[26,27] when the metal dispersed over the support is used as a catalyst for the growth of carbon nanotubes. These are described as follows.

Base growth mechanism. When there is a strong interaction between the metal and support, then this mechanism is assumed to be adopted for the growth of CNT. When there exists a strong interaction between the metal and support the hydrocarbon molecule which is used as the source of the carbon for the growth of carbon nanotubes cannot lift the metal particle from the support. Then the tube grows away from the metal particle which is deposited on the surface of the support.[28] Here the metal particle helps only in the nucleation of the CNT.

Tip growth mechanism. When there is a weak interaction between the metal and the support then the growth of CNT follows this mechanism. In this case the metal particle which is loosely bonded to the support will be lifted by the carbon source molecule and the catalyst remains at the tip of the developing nanotube.

In the present study the growth mechanism is assumed to follow the tip growth mechanism, because it is clearly observed

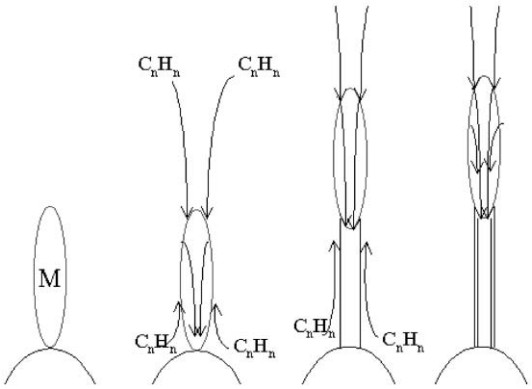

Fig. 9 Schematic representation of the tip growth mechanism.

from the HRTEM results (see Fig. 5) that metal particle is present at the tip of the tube. In this case, which is represented schematically in Fig. 9, initially the acetylene molecule approaches the metal catalyst particle and undergoes decomposition at the contact of the metal and support. Thus formed metastable carbon diffuses through the metal particle, simultaneously lifting the metal catalyst particle, as there exists a weak interaction between the metal cobalt and the support zeolite beta. Then the tube grows continuously by using the metastable carbon which is formed by the decompostion of the acetylene at the tip of the tube. This carbon diffuses through the metal catalyst particle and forms the inner walls of the multiwalled CNT as depicted in Fig. 9. The diameter of the tube is also dependent on the topography of the metal particle and the facet in which it is deposited over the support. Due to this reason we observe the formation of the carbon nanotubes in a given range of diameters as described earlier in the paper. However in some cases[29] we also observed a metal particle embedded in to the walls of the tubes and in the inner cores of the carbon nanotube. The growth mechanism in those cases is still not clearly understood.

Conclusion

In conclusion, we have successfully demonstrated here for the first time an alternative support, zeolite beta in the presence of metal cobalt particles, for the synthesis of multiwalled carbon nanotubes. The yields of carbon nanotubes are comparable with those of the literature results. SQUID magnetic measurements explain that these Co-nanotubes exhibits very good ferromagnetism. From the TEM results we have proposed a tip growth mechanism for the formation of multiwalled carbon nanotubes using cobalt metal particles as catalyst and zeolite beta as support in vapour phase.

Acknowledgement

GK thanks NSC, ROC for the award of postdoctoral fellowship through a grant of NSC 89-2113-M-003 and IAMS for the hospitality. We thank Prof. Kuei-Hsien Chen, IAMS for HRTEM.

References

1 S. Iijima and T. Ichihashi, *Nature (London)*, 1993, **363**, 603.
2 A. Thess, R. Lee, P. Nikolaev, H. J. Dai, P. Petit, J. Robert, C. H. Xu, Y. H. Lee, S. G. Kim, A. G. Rinzler, D. T. Colbert, G. E. Scuseria, D. Tomanek, J. E. Fisher and R. E. Smalley, *Science*, 1996, **273**, 483.
3 C. Journet, W. K. Maser, P. Bernier, A. Loiseau, M. L. De La Chapelle, S. Lefrant, P. Deniart, R. Lee and J. E. Fisher, *Nature*, 1997, **388**, 756.
4 H. W. Kroto, J. R. Heath, S. C. O'Brien, R. F. Curl and R. E. Smalley, *Nature*, 1985, **318**, 162.
5 P. Bernier, D. Laplaze, L. Barnedette, J. Mlambert, G. Flamant, M. Lebbrun, A. Brunnelle and S. Della-Negra, *Synth. Met.*, 1995, **70**, 1455.
6 D. Laplaze, P. Bernier, L. Barnedette, J. Mlambert, G. Flamant, M. Lebbrun, A. Brunnelle and S. Della-Negra, *Synth. Met.*, 1997, **86**, 2295.
7 W. K. Hsu, J. P. Hare, M. Terrones, H. W. Kroto, D. R. M. Walton and P. J. F. Harris, *Nature*, 1995, **377**, 687.
8 W. K. Hsu, M. Terrones, J. P. Hare, H. Terrones, H. W. Kroto and D. R. M. Walton, *Chem. Phys. Lett.*, 1996, **262**, 161.
9 W. S. Cho, E. Hamada, Y. Kondo and K. Takayanagi, *Appl. Phys. Lett.*, 1996, **69**, 278.
10 Y. L. Li, Y. D. Yu and Y. Liang, *J. Mater. Res.*, 1997, **12**, 613.
11 W. Z. Li, S. S. Xie, L. X. Qian, B. H. Chang, B. S. Zou, W. A. Zhou, R. A. Zhao and C. Wang, *Science*, 1996, **274**, 1701.
12 A. Fonseca, K. Herandi, P. Peidigrosso, J.-F. Colomer, K. Mukhopadhyay, R. Doome, S. Lazarescu, L. P. Biro, P. H. Lambin, P. A. Thiry, D. Bernaerts and J. B. Nagy, *Appl. Phys. A*, 1998, **67**, 11.
13 A.K Sinha, D. W. Hwang and L.-P. Hwang, *Chem. Phys. Lett.*, 2000, **332**, 455.
14 N. Wang, Z. K. Tang, G. D. Li and J. S. Chen, *Nature*, 2000, **408**, 50.
15 Z. K. Tang, H. D. Sun, J. Wang, J. Chen and G. Li, *Appl. Phys. Lett.*, 1998, **73**(16), 2287.
16 R. W. Wadlinger, G. T. Kerr and E. J. Rosinski, *US Patent* No.3, 308, 069, Mobil Oil Corporation, 1967.
17 R. T. K. Baker and P. S. Harris, *Formation of filamentous Carbon in Chemistry and Physics of Carbon*, Marcel Dekker, New York, 1978, vol. 14, p. 83.
18 R. T. K. Baker, *Carbon*, 1989, **27**, 315.
19 F. J. Derbyshire, A. E. B. Persland and D. L. Trimm, *Carbon*, 1975, **13**, 111.
20 X. X. Zhang, G. H. Wen, S. Huang, L. Dai, R. Gao and Z. L. Wang, *J. Magn. Magn. Mater.*, 2001, **231**, L9.
21 S. Liu, J. Zhu, Y. Mastai, I. Felner and A. Gedanken, *Chem. Mater.*, 2000, **12**, 2205.
22 K. Lafdi, A. Chin, N. Ali and J. F. Despres, *J. Appl. Phys.*, 1996, **79**(8), 6007.
23 N. Grobet, W. K. Hsu, Y. Q. Zhu, J. P. Hare, H. W. Kroto, D. R. M. Walton, M. Terrones, H. Terrones, P. H. Redlich, M. Ruhle, R. Escuder and F. Morales, *Appl. Phys. Lett.*, 1999, **75**(21), 3363.
24 T. Hayashi, *Nature*, 1996, **381**, 772.
25 S. Liu, X. Tang, Y. Mastai, I. Felner and A. Gedanken, *J. Mater. Chem.*, 2000, **10**, 2502.
26 S. Amelinckx, X. B. Zhang, D. Bernaerts, X. F. Zhang, V. Ivanov and J. B. Nagy, *Science*, 1994, **265**, 635.
27 M. Yudasaka, R. Kikuchi, Y. Ohi, E. Ota and S. Yoshimua, *Appl. Phys. Lett.*, 1997, **70**, 1817.
28 S. Fan, M. G. Chapline, N. R. Franklin, T. W. Tombler, A. M. cassell and H. Dai, *Science*, 1999, **283**, 512.
29 A.K Sinha, D. W. Hwang and L. P. Hwang, unpublished results.